PHYSICAL REVIEW B VOLUME 20, NUMBER 12 15 DECEMBER 1979

Negative magnetoresistance of pregraphitic carbons

A. A. Bright*
Union Carbide Corporation, Carbon Products Division, Parma Technical Center, P. O. Box 6116, Cleveland, Ohio 44101
(Received 29 March 1979)

A theory of the magnetoresistance of disordered carbons is presented and applied to experimental results on carbon fibers and glassy carbon. The important features of the model include (a) a two-dimensional band structure and density of states, (b) a shallow acceptor level due to defects, (c) collision-broadened Landau levels, and (d) an extra density of states in the $m = 0$ Landau level to account for the effects of partial three-dimensional ordering of the graphitelike layers. The negative magnetoresistance results from field-induced changes in the density of states which lead to an increase in the carrier concentration with field. Four structure-dependent parameters are used to fit the resistivity as a function of temperature, field strength, and orientation of the sample in the field. Approaches to improving the model are discussed.

I. INTRODUCTION

Although the electronic properties of graphite are now reasonably well understood, the same level of understanding has not been reached for pregraphitic, i.e., partially ordered, carbons. Qualitative discussions have been presented[1] to describe the changes in the band structure as the physical structure evolves from a disordered, glassy state to a highly ordered or graphitic state, but they have for the most part been unable to provide a quantitative description of the electronic properties. One of the principal outstanding problems is the negative magnetoresistance observed in these materials at low temperatures.[2] Numerous attempts have been made to explain this phenomenon,[2-5] using virtually all of the available theories of negative magnetoresistance. A summary of this situation is presented in Ref. 2, where it is conclused that none of the theories is adequate for the case of carbon.

The present paper describes a new theory of the magnetoresistance of carbons which has been developed as part of a program to investigate the electronic properties of mesophase pitch-based carbon and graphite fibers.[6] Some of the central features of this theory are drawn from the work of Yazawa, who attempted to explain the magnetoresistance[5] and Hall effect[7] of carbons on the basis of a two-dimensional band-structure model. It is, in fact, quite natural to start from a two-dimensional model for disordered carbons such as these. The three-dimensional correlations between layer planes, which are characteristic of perfect crystalline graphite, are absent in disordered carbons.[1] As the structure evolves toward the graphitic state, the "crystallite size," or size of coherently oriented regions, increases. Simultaneously, the interlayer correlations gradually increase so that interlayer interactions gradually start to play an important role in the band structure. For glassy carbon, carbon fibers, and similar disordered carbons, however, the lack of extensive interlayer ordering implies that the three-dimensional effects on the band structure may be neglected in the first approximation, and a two-dimensional band structure is an appropriate starting point.

Yazawa's model, however, contained several errors, internal inconsistencies, and physically unreasonable features which prevented him from achieving quantitative agreement with the experimental data. The theory presented here describes quantitatively the magnetoresistance of fibers having structures ranging from glassy to highly graphitic as a function of temperature and of magnetic field strength and orientation, as well as the magnitude and temperature dependence of the resistivity. When extended to the low-mobility limit, the theory provides a good description of the magnetoresistance of bulk glassy carbon.[8] The parameters of the theory are related to structural parameters of the material and can provide information about the evolution of the structure of fibers from glassy to graphitic as the processing temperature is increased. This information is in good agreement with x-ray observations on the same samples.[6] The theory may be applied equally well to other forms of pregraphitic carbons.

II. EXPERIMENTAL

The experimental procedures have been described in detail elsewhere.[6] Briefly, resistivity and magnetoresistance measurements were made on single carbon filaments using ac and dc four-probe techniques. Contacts were made with silver paint to four 0.0254-mm diameter copper wires attached to insulated copper blocks. Samples were mounted, six at a time, in an Air Products and Chemicals Helitran cryostat for measurements from room temperature down to 4.2 K. The cryostat was mounted between the poles of a 12-in. electro-

magnet capable of fields up to 1.4 T. The cryostat could be rotated in the field for orientation-dependence studies.

III. THEORY

As in Yazawa's theory,[5,7] we assume that the electronic structure is described by the two-dimensional simplification of the Wallace model. The Landau-level structure for this two-band model was calculated by McClure[9] and is shown in Fig. 1. The Landau levels are located at energies (in SI units)

$$E_m=\pm(\tfrac{3}{2})^{1/2}\gamma_0 a_0\left(\frac{eH}{\hbar}\right)^{1/2}\sqrt{m},\quad m=0,1,2,\ldots \tag{1}$$

and the density of states in each level is

$$g_m=\frac{4eH}{\pi c_0\hbar}\equiv AH. \tag{2}$$

Here γ_0 is the in-plane interaction between nearest neighbors, a_0 and c_0 are the lattice constants, and H is the magnetic field component perpendicular to the layer planes.

An acceptor level of localized defect states at energy $E_a\sim-0.01$ eV and density N_a is assumed, which lowers the Fermi energy slightly into the valence band. To approximate the effect of a small amount of three-dimensional ordering, which produces a slight band overlap, an excess density of states N_0 is added to the $n=0$ Landau level as shown in Fig. 1. This approximation will be discussed in detail in Sec. V.

In addition to these approximations used by Yazawa, we have incorporated several additional features in the model which are essential for good quantitative agreement with the experimental results. Most important of these is the collision broadening of the Landau levels as a result of defect scattering. This has the effect not only of eliminating the Schubnikov-deHaas oscillations (which are not observed experimentally) but also of producing better numerical agreement with experiment using reasonable parameter values. The effect on the density of states is evident in Fig. 1. If we assume for mathematical convenience a Gaussian form for the broadened levels, the density of states is given by the expression

$$g(E)=\frac{AH\lambda}{\pi}\left[\left(1+\frac{N_0}{AH}\right)\exp(-\lambda^2E^2)+\sum_{m=1}^{\infty}\{\exp[-\lambda^2(E-E_m)^2]+\exp[-\lambda^2(E+E_m)^2]\}\right], \tag{3a}$$

where λ^{-1} represents the width of each level and is related to the zero-field mobility μ by

$$\lambda^{-1}=\frac{1}{\sqrt{\ln 2}}\left[\left(\frac{\hbar e}{\mu m^*}\right)^2+(k_BT)^2\right]^{1/2}. \tag{3b}$$

In this equation, it is assumed for simplicity that $\mu=e\tau/m^*$, where m^* is an average effective mass arbitrarily set equal to 0.025 times the free-electron mass. It is also assumed that the relaxation times for conduction and for Landau-level broadening are equal. These assumptions affect primarily the precise numerical value of λ for a given μ rather than the functional form of the relationship. Changes in λ will affect the numerical results to a small degree but will have no essential effect on the general features of the model. A thermal-broadening term is included as well as the collision-broadening term, since it was found that the use of the Fermi function alone [in Eqs. (4) and (5)] did not account completely for thermal effects; the latter procedure resulted in resolved Schubnikov-deHaas oscillations at high temperatures for high-mobility values.

The electron and hole concentrations n and p are given by

$$n=\int_0^{\infty}\frac{g(E)dE}{1+\exp[(E-\eta)/kT]} \tag{4a}$$

and

$$p=\int_0^{\infty}\frac{g(E)dE}{1+\exp[(E+\eta)/kT]}, \tag{4b}$$

where the Fermi energy η is determined self-consistently from the neutrality condition

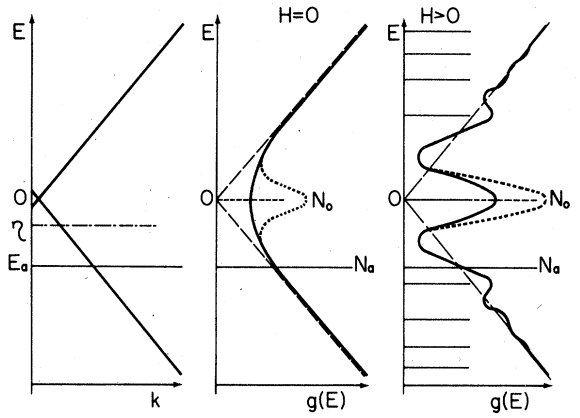

FIG. 1. Band structure $k(E)$ and density of states $g(E)$ without and with an applied magnetic field. Asymptotes (long dashes) indicate zero-field density of states in the absence of collision broadening. Positions of Landau levels are indicated by solid lines. Short dashes indicate additional density of states N_0 included in $m=0$ level to account for band overlap. Other symbols are defined in the text.

$$p-n-\frac{N_a}{1+\exp[(E_a-\eta)/kT]}=0. \tag{5}$$

A number of alternative definitions of n and p were tried, since Eqs. (4a) and (4b) appear to treat the low-energy tails of electron peaks and high-energy tails of hole peaks in an arbitrary way. The given expressions were, however, most successful in fitting the experimentally observed behavior and can be justified as follows: If we take the band structure as well defined (i.e., $E(k)$ is not broadened but describes states with well-defined energies between which scatterings can occur), then it is impossible for electrons to have negative energies or for holes to have positive energies. The broadening of the density of states is merely a way of expressing the range of levels into which scatterings can occur. (This is different from the case of amorphous semiconductors, in which the energies become uncertain due to fluctuations in density or composition, leading to band tailing into the forbidden gap.) Since electrons cannot scatter into holes, only positive energies can be used for electrons and negative energies for holes.

We set the ratio of the electron and hole mobilities (in the absence of a magnetic field) equal to unity, since its value is unknown, and the calculation is not very sensitive to the exact value. We assume that the field has no effect on the scattering mechanism nor on the effective mass. The (field-dependent) electron and hole concentrations n and p are used explicitly within the standard expressions for the conductivity tensor components,

$$\sigma_{xx}(H)=(n+p)e\mu/[1+(\mu H)^2] \tag{6a}$$

and

$$\sigma_{xy}(H)=(p-n)e\mu^2H/[1+(\mu H)^2], \tag{6b}$$

in determining the field dependence of the conductivity.

The resulting expression for the resistivity is

$$\rho(H)=\frac{1+\mu^2H^2}{(p+n)e\mu\left[1+\left(\frac{p-n}{p+n}\right)^2\mu^2H^2\right]} \tag{7}$$

and for the magnetoresistance

$$\frac{\Delta\rho}{\rho_0}=\frac{-1+\left(\frac{p_0+n_0}{p+n}\right)\left[1+\mu^2H^2\left(1-\frac{(p-n)^2}{(p+n)(p_0+n_0)}\right)\right]}{1+\left(\frac{p-n}{p+n}\right)^2\mu^2H^2}, \tag{8}$$

where the subscript zero indicates the zero-field value. In the limit of $n=0$, this expression reduces to

$$\frac{\Delta\rho}{\rho_0}=\frac{p_0}{p}-1, \tag{9}$$

reflecting the fact that a single-band system has no magnetoresistance if the carrier concentration is field independent. Yazawa[5] used a two-band expression, appropriate for the case $n=p$, even when $n\ll p$, leading to serious errors in his magnetoresistance curves. The formula used by Yazawa also implicitly made the approximation $\rho_{xx}=1/\sigma_{xx}$. This approximation is valid only when $\sigma_{xy}\ll\sigma_{xx}$, or $\mu H\ll 1$, a condition not always true for relevant field values.

The final step in the calculations is to integrate Eq. (8) over the angular orientation distribution of crystallites in the fiber or glassy carbon sample. For the highly aligned structure of the fibers used in this study as well as for the isotropic glassy carbon, it was found that a simple average of the resistivities of individual crystallites was sufficiently accurate, since the magnitude of the magnetoresistance was small. In fact, no significant differences in the results were evident when the conductivities were averaged instead of the resistivities. The "true" behavior lies somewhere between these two extremes. The angular distribution of the crystallite c axes in the fibers is assumed to be Gaussian with respect to the polar angle θ between the c axis and the fiber axis, peaked at $\theta=\pi/2$, and isotropic with respect to the transverse orientation.

We now consider more specifically the case of glassy carbon. The mobility in this case is somewhat lower; therefore it is necessary to reexamine the density-of-states function $g(E)$ in this limit of low mobilities. Equation (3) shows that g is a sum of Gaussians, centered at energies E_m which depend on the magnetic field and with widths inversely proportional to the mobility. At low fields or low mobilities, the number of terms needed in this sum is large, and it is more convenient to expand g in powers of H. The result is

$$g(E,H)=\frac{\lambda\exp(-\lambda^2E^2)}{\sqrt{\pi}}\times\left(N_0+\frac{2A}{\lambda^2B}+\frac{4AE}{\lambda B}\exp(\lambda^2E^2)\,\mathrm{erf}(\lambda E)-\frac{2A}{\lambda^2B}\sum_{k=2}^{\infty}\frac{B_k}{k}(\lambda^2BH)^k\frac{H_{2k-2}(\lambda E)}{(2k-2)!}\right), \tag{10}$$

where B_k is the kth Bernoulli number, $H_i(\lambda E)$ is a Hermite polynominal, $\mathrm{erf}(\lambda E)$ is the error function, and

$$B\equiv\tfrac{3}{2}\gamma_0^2a_0^2\frac{e}{\hbar}. \tag{11}$$

Only even powers of H enter into this expression, since the odd-order Bernoulli numbers are all zero. The range of validity of this expansion depends on the mobility through λ. For low mobilities, say, $\mu\sim 0.10$ m^2/V s, the expansion can be

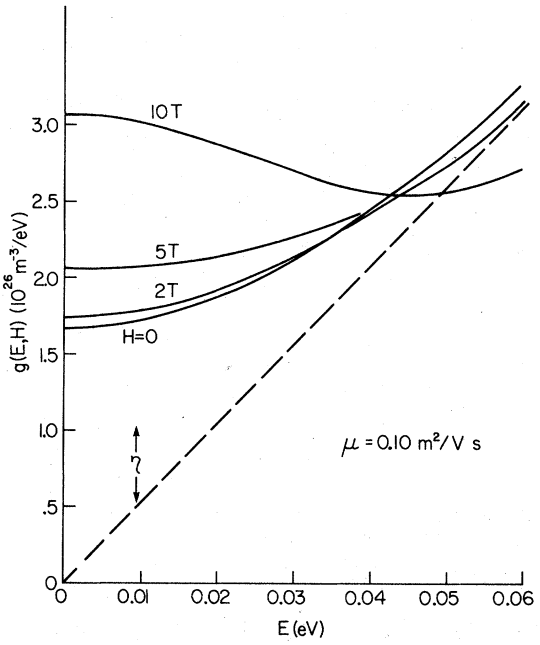

FIG. 2. Density of states as a function of energy for various magnetic field strengths and a mobility of 0.10 m^2/Vs. The dashed line indicates the zero-field density of states in the absence of collision broadening. The approximate position of the Fermi energy is indicated by η.

terminated at the H^4 term with negligible error for fields up to 1.5 T. As shown in Fig. 2, at all energies up to the Fermi energy the effect of small fields is, roughly, to increase g uniformly by an amount proportional to H^2. It is only at much higher fields that resolvable Landau levels begin to be evident.

The following approximate derivation is helpful in understanding the field dependence of the negative magnetoresistance in glassy carbon. The calculations presented in Sec. IV were, however, performed using the full formalism of the theory without the approximations made here. We assume, first, that only the hole band is occupied, so the magnetoresistance is given by Eq. (9). Second, for all energies up to the Fermi energy, λE is small and $g(E,H) \cong g(0,H)$. Third, at sufficiently low temperatures ($kT \ll \eta$), p is proportional to g; finally, at low temperatures, λ is proportional to μ. Then, terminating the expansion of g at the H^2 term,

$$g = a + bH^2, \tag{12a}$$

where

$$a = \frac{\lambda \exp(-\lambda^2 E^2)}{\sqrt{\pi}} \left(N_0 + \frac{2A}{\lambda^2 B} \right) \tag{12b}$$

and

$$b = \exp(-\lambda^2 E^2) A B \lambda^3 / 6\sqrt{\pi} \,. \tag{12c}$$

The fractional change in g is

$$\frac{g(0,0)}{g(0,H)} = \frac{a}{a+bH^2} \cong 1 - \frac{b}{a} H^2, \tag{13}$$

and the resulting magnetoresistance is

$$\frac{\Delta\rho}{\rho_0} = -\frac{b}{a} H^2 = \frac{-AB\lambda^2 H^2/6}{N_0 + 2A/\lambda^2 B}$$

$$= \frac{-1.67\times10^{19}\mu^2}{N_0 + 1.63\times10^{17}/\mu^2} H^2 \cong -102\mu^4 H^2, \tag{14}$$

where μ is in $m^2/V\,s$ and H is in T.

The mechanism for the negative magnetoresistance resulting from these calculations is most clearly seen in the quantum limit, which occurs at fields of order 0.2 T or less, but is valid at lower fields as well, since all occupied levels are included in the calculation. In the quantum limit, only the lowest ($m = 0$) Landau level is occupied. Since the density of states in this level is proportional to the magnetic field component perpendicular to the layer planes, the number of charge carriers increases rougly linearly with field, leading to a decrease in the resistivity. At lower fields, the broadened levels result in a structureless density of states. The calculation above shows that this density of states increases roughly uniformly (at low energies) with the square of the magnetic field, resulting in a quadratic dependence of the carrier concentration on field and a quadratic negative magnetoresistance. However, in sufficiently well-graphitized samples ($p - n \ll p + n$) the $\mu^2 H^2$ term in the numerator of Eq. (8) dominates, and the magnetoresistance is positive. In intermediate cases, the magnetoresistance is negative at low fields and positive at high fields. This behavior results partly from the competition between the negative linear and positive quadratic terms and partly from the fact that the Fermi level shifts toward zero energy as the field increases, thereby increasing the electron concentration n and making the $\mu^2 H^2$ term more significant.

IV. RESULTS

Typical results for the transverse magnetoresistance of various fibers at 4.2 K are shown in Fig. 3. A flexible simplex-type least-squares-fitting routine[10] was used to optimize the values of the adjustable parameters: N_0, the density of states added to the $n = 0$ Landau level; N_a, the acceptor concentration; μ, the zero-field mobility; and E_a, the acceptor energy. The values of these parameters are given in Table I along with the χ^2 values (normalized to the mean square of the data for each sample). The parameters vary regularly and essentially monotonically as the degree of

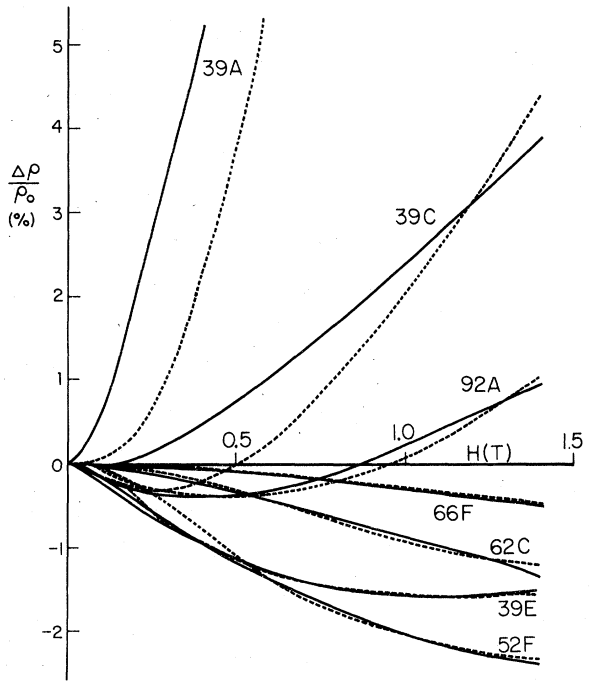

FIG. 3. Transverse magnetoresistance at 4.2 K for typical carbon fiber samples processed at temperatures from 1700 to 3000 °C. Solid lines: experimental results. Dashed lines: calculated least-square fits.

graphitic order increases. As expected, the most graphitic samples have the highest mobilities, the largest N_0, and the smallest defect concentrations. The numerical values are reasonable and consistent with the assumptions of the model. It should be noted in particular that N_a is of order 10^{24} m^{-3}, consistent with localized defect states, whereas Yazawa[5] found much higher values of N_a of order 10^{27} m^{-3}. The calculation is insensitive to the value of E_a in the most graphitic cases, since the defect level is far below the Fermi level. The measured and calculated resistivities were required to agree within 10% for each sample. The quality of the fit is not as good at high processing temperatures as at low ones because the increasing three-dimensional order makes the two-dimensional approximation used in the model less suitable.

The variation of the magnetoresistance with angle between the fiber axis and the field is correctly given by the theory as shown in Fig. 4. The fitted parameters were determined for the transverse (90°) orientation. These values were then used to generate the magnetoresistance curves for the other orientations varying only the orientation angle.

The temperature dependence of the resistivity and of the magnetoresistance of fibers can be fitted allowing the mobility to vary with temperature while holding the other parameters fixed. The fitted values of the mobility are consistent with a scattering rate consisting of a constant (defect-limited) term plus a temperature-dependent (phonon) term with an exponent of about 1. This temperature dependence is in agreement with expectations based on the low-temperature mobility value and the observed temperature dependence for graphite specimens of various degrees of perfection.[11]

Figure 5 shows the relation between the model parameters and the structural features of the fibers as determined by x-ray studies. The band overlap parameter N_0 is plotted against the ratio of the intensities of the (112) and (110) x-ray powder diffraction lines. This ratio is a convenient measure of the extent of three-dimensional ordering in carbons, since the (110) line is an in-plane line which is unaffected by the presence of interlayer correlations, whereas the (112) line depends on the precise interlayer correlations of three-dimensional graphite. For perfect graphite, the intensity ratio $I(112)/I(110)$ is about 1.6. A monotonic relationship between N_0 and the three-dimensional order is evident in Fig. 5.

Figure 6 shows the defect concentration N_a plotted against the crystallite size, estimated in this case by L_c, the stack height of layer planes. L_c is determined from the width of the (002) and (004)

TABLE I. Values of fitted parameters and χ^2 (normalized) for several carbon-fiber samples.

Sample	Processing temp., °C	ρ(4.2 K), $\mu\Omega$m Meas.	Calc.	N_o 10^{24} m^{-3}	N_a 10^{24} m^{-3}	E_a eV	μ m^2*V s	χ^2_{norm}
29*A*	3000	3.79	3.92	19.2	1.1	−0.013	1.110	0.0371
39*C*	3000	5.08	4.88	9.1	1.1	−0.0058	1.150	0.0495
92*A*	3000	7.00	6.56	6.0	0.9	−0.0043	1.040	0.0351
39*E*	3000	6.62	6.80	4.5	1.6	−0.0075	0.567	0.00555
52*F*	2500	6.77	6.72	5.8	2.6	−0.0118	0.371	0.00483
62*B*	2000	9.30	9.23	5.0	2.7	−0.0154	0.255	0.00476
62*C*	2000	9.24	9.18	5.4	3.2	−0.0182	0.213	0.00473
66*F*	1700	12.45	11.80	5.5	3.5	−0.0193	0.152	0.00348

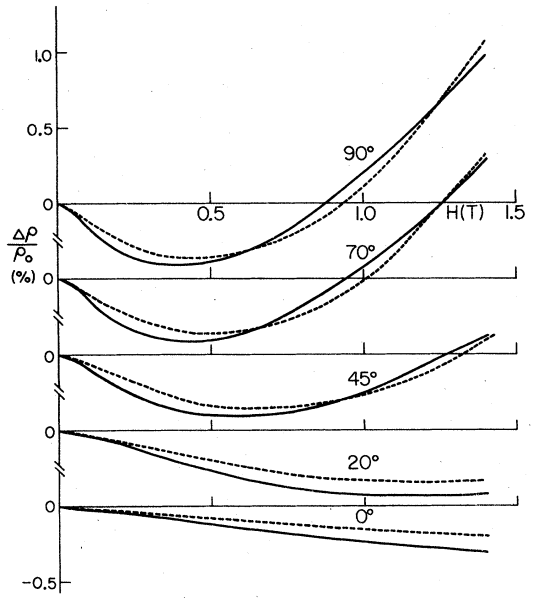

FIG. 4. Dependence of magnetoresistance at 4.2 K on orientation in the magnetic field. Fitted parameters were determined in the transverse orientation (90°). Solid lines: experimental results. Dashed lines: calculated fits.

powder diffraction lines. As is clear, the defect concentration and the crystallite size are related inversely, as expected; the magnitude of N_a is appropriate for these crystallite dimensions.

There is insufficient experimental or theoretical information on the electronic structure of defects in graphite to judge whether the variation of E_a with the degree of structural order is realistic. It is, of course, possible that this apparent variation is a consequence of the simplifying assumption of a single defect level rather than a distribution of levels. In the absence of detailed information on the defect states in these materials, the inclusion of additional adjustable parameters to specify a distribution of defect levels would yield no useful new information and would not increase the ability of the model to fit the experimental results. In any case, the calculation is insensitive to the value of E_a when the defect level is several times kT below the Fermi level, as is true for the more highly graphitized materials.

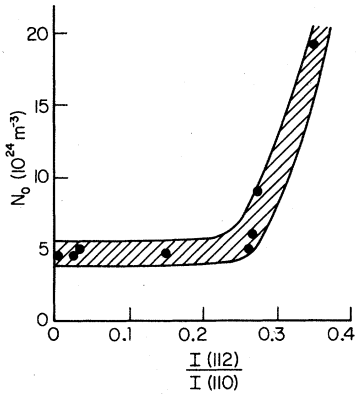

FIG. 5. Relation between the band overlap parameter N_0 and the degree of three-dimensional order determined by the ratio of intensities of the (112) and (110) x-ray diffraction lines.

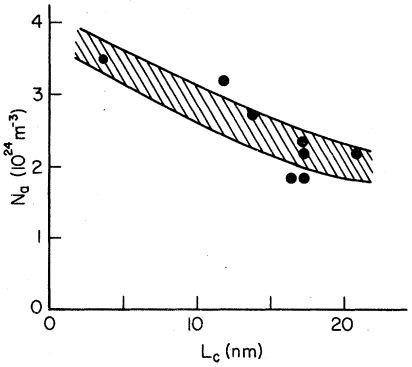

FIG. 6. Dependence of defect concentration on crystallite size as represented by the layer stack height L_c.

Magnetoresistance data on glassy carbon samples were supplied by Bragg.[12] Least-squares fits were performed on data for a sample processed for two hours at 2300 °C and, after processing, measured at various temperatures up to 100 K. The results are shown in Fig. 7, where the fits can be seen to be very good. At each temperature the value of the zero-field resistivity was required to agree with the measured value within 20%.

Table II lists the values of the fitted parameters at each temperature. Looking first at N_a and E_a, we see that they are not constant, as might be assumed at first. However, it must be kept in mind that there is, in fact, a distribution of defect-state energies, and the use of N_a and E_a to represent this distribution is an approximation. The distribution of occupied defect states is temperature dependent; so the changes in N_a and E_a here are not surprising. In particular, the increase in N_a at the higher temperatures is what one would expect in this context. This effect is much less apparent in the fiber results because the more ordered structures of the fibers results in a narrower distribution of defect states.

The temperature dependence of the mobility is of particular interest. This is shown in Fig. 8. We see that initially μ varies as $T^{-1/4}$. This is interesting in light of the observation by Saxena and Bragg[8] that the magnetoresistance of these samples was a single function of $H/T^{1/2}$. Recalling the approximate expression for the magnetoresistance

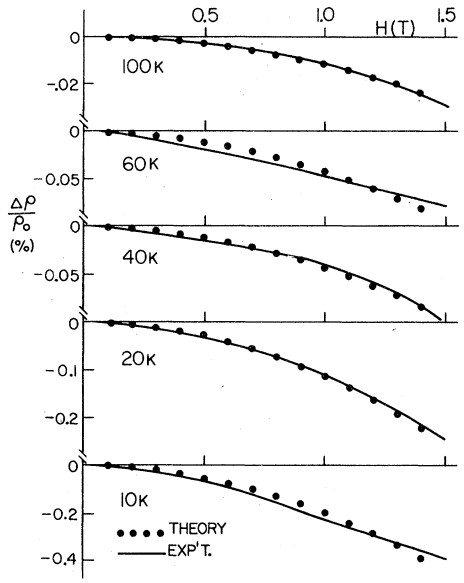

FIG. 7. Magnetoresistance of glassy carbon heated at 2300 °C for 2 h measured at temperatures from 10 to 100K. Solid lines: experimental results. Dotted lines: calculated fits.

as proportional to $\mu^4 H^2$, we see that this dependence on $H/T^{1/2}$ occurs quite naturally in this theory.

V. DISCUSSION

The model described here appears to work well in the regime of graphitization prior to the onset of three-dimensional ordering where a negative magnetoresistance is observed. At higher processing temperatures the increased ordering between layer planes leads to significant changes in the band structure and the magnetoresistance becomes positive. The model gives much poorer quality fits in this region.

It should be possible, however, to extend the model to account for three-dimensional effects by explicitly including the changes in the band structure due to interlayer interactions. The Slonczewski-Weiss-McClure band-structure model for

TABLE II. Values of fitted parameters for a glassy carbon sample at several temperatures.

T K	N_0 10^{24} m^{-3}	10^{24} m^{-3}	E_a eV	μ m^2/V s
10	8.9	8.6	−0.0101	0.1015
20	10.4	8.4	−0.0096	0.0901
40	10.8	9.2	−0.0097	0.0737
60	10.1	8.6	−0.0087	0.0863
100	5.4	12.8	−0.0100	0.0786

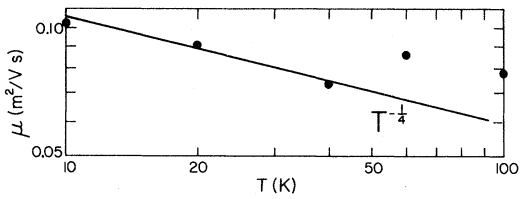

FIG. 8. Fitted mobility values for the glassy carbon data in Fig. 7 as a function of temperature.

graphite[13] describes the bands near the Fermi level in terms of seven tight-binding parameters. In the two-dimensional case, all but one of these seven parameters are set equal to zero. The next stage of approximation is a four-parameter theory.[11] It seems reasonable to suppose that the beginning stages of three-dimensional order can be accounted for by using this four-parameter model with the parameters which were zero in the two-dimensional case "turned on" slowly toward their values in single-crystal graphite. Figure 9 shows how this happens.

In these curves, the Landau levels are shown as a function of k_z from zero to the top surface of the Brillouin zone. In the two-dimensional case, there is, of course, no k dispersion. As the band parameters are turned on to 1% of the graphite values, some dispersion starts to develop and the degeneracy of the levels is split. By 3%, the dispersion is increasing significantly, but the bands still look more like the two-dimensional than the three-dimensional case. By using this approach, a more realistic density-of-states curve could be generated, which might extend the region of validity of the model to more highly graphitic sam-

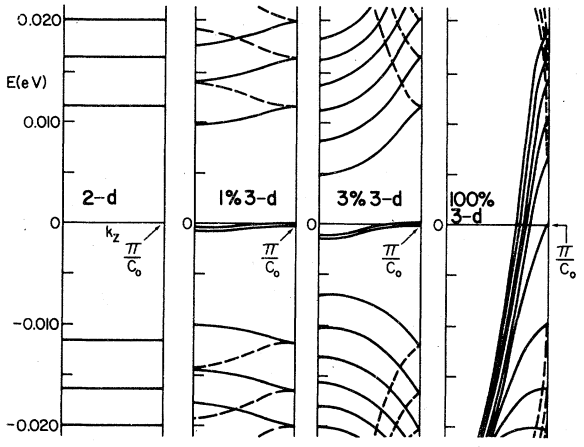

FIG. 9. Landau-level dispersion for two-dimensional, mixed, and three-dimensional graphite. The magnetic field strength is 0.10 T. The two-dimensional levels are doubly degenerate. Only the first few three-dimensional levels are shown for clarity.

ples.

These curves also offer some insight into the reasons why the parameter N_0 is successful in approximating the three-dimensional ordering. It looks at first as if the simple procedure of adding extra density to the $m = 0$ Landau level would be too crude to work well. But these Landau-level curves show that the dashed levels rapidly move to high energies and become well separated from the Fermi energy, while the solid levels remain relatively unchanged. The important thing is that the $m = 0$ level degeneracy is almost not split at all, so that this level effectively has twice the density of the others. The magnitude of N_0 is roughly the same as the density in the two-dimensional levels; therefore it is clear now why the approximation is successful. There are, of course, differences in the details of the handling of the levels in the approximate and the more exact calculations. Modification of the calculation to account for these differences would be expected to result in an improved ability of the model to duplicate the experimental results.

VI. SUMMARY AND CONCLUSIONS

The model described here has been shown to provide a good fit to magnetoresistance data at low magnetic fields ($H < 1.4$ T) for a wide varlety of carbon fiber samples, ranging from highly graphitic to very poorly ordered, as well as glassy carbon. By using four adjustable parameters, it is possible to fit simultaneously the magnitude and temperature dependence of the resistivity and the dependence of the magnetoresistance on field strength, orientation, and temperature. The model should be capable of explaining other electronic properties as well, such as the Hall effect and the magnetic susceptibility. No attempt has yet been made to do so because of a lack of the relevant experimental data on the present samples.

The assumptions used in the model are natural and reasonable. No arbitrary, impurity-dependent or sample-dependent features are required. Thus, the model should be successful for essentially any type of disordered carbon, whether graphitizable or not.

The values of the parameters of the theory are directly related to the structure of the sample. It is straightforward to use the parameter values obtained by analyzing the magnetoresistance to investigate the evolution of the samples as graphitization progresses.

ACKNOWLEDGMENTS

The author wishes to thank Dr. J. A. Woollam for making available the computer facilities of the NASA Lewis Research Center, Dr. W. F. Ford for assisting with the computer programming, and Professor R. H. Bragg for supplying the glassy carbon data. The author acknowledges useful discussions with Professor I. L. Spain and Professor J. W. McClure.

---

*Present address: IBM Corporation, T. J. Watson Research Center, Yorktown Heights, New York 10598.

[1]S. Mrozowski, Carbon 9, 97 (1971).
[2]P. Delhaes, P. de Kepper, and M. Uhlrich, Philos. Mag. 29, 1301 (1974).
[3]S. Yugo, J. Phys. Soc. Jpn. 34, 1421 (1973).
[4]S. Fujita, Carbon 6, 746 (1968).
[5]K. Yazawa, J. Phys. Soc. Jpn. 26, 1407 (1969).
[6]A. A. Bright and L. S. Singer, Carbon 17, 59 (1979).
[7]K. Yazawa, J. Chim. Phys. 64, 961 (1967).
[8]R. R. Saxena and R. H. Bragg, Philos. Mag. 36, 1445 (1977).
[9]J. W. McClure, Phys. Rev. 104, 666 (1956).
[10]C. D. Hendrix, private communication.
[11]I. L. Spain, in *Chemistry and Physics of Carbon*, edited by P. L. Walker and P. A. Thrower (Dekker, New York, 1973), Vol. 8, p. 105.
[12]R. H. Bragg, private communication.
[13]J. C. Slonczewski and P. R. Weiss, Phys. Rev. 109, 272 (1958); J. W. McClure, Phys. Rev. 108, 612 (1957).